Research

MS1/MMD1 homologues in the moss *Physcomitrium patens* are required for male and female gametogenesis

Katarina Landberg (ID), Mauricio Lopez-Obando (ID), Victoria Sanchez Vera (ID), Eva Sundberg (ID) and Mattias Thelander (ID)

Department of Plant Biology, The Linnean Centre of Plant Biology in Uppsala, Swedish University of Agricultural Sciences, PO Box 7080, SE-75007 Uppsala, Sweden

Author for correspondence:
Mattias Thelander
Email: mattias.thelander@slu.se

Summary

• The Arabidopsis Plant HomeoDomain (PHD) proteins AtMS1 and AtMMD1 provide chromatin-mediated transcriptional regulation essential for tapetum-dependent pollen formation. This pollen-based male gametogenesis is a derived trait of seed plants. Male gametogenesis in the common ancestors of land plants is instead likely to have been reminiscent of that in extant bryophytes where flagellated sperms are produced by an elaborate gametophyte generation. Still, also bryophytes possess MS1/MMD1-related PHD proteins.
• We addressed the function of two MS1/MMD1-homologues in the bryophyte model moss *Physcomitrium patens* by the generation and analysis of reporter and loss-of-function lines.
• The two genes are together essential for both male and female fertility by providing functions in the gamete-producing inner cells of antheridia and archegonia. They are furthermore expressed in the diploid sporophyte generation suggesting a function during sporogenesis, a process proposed related by descent to pollen formation in angiosperms.
• We propose that the moss MS1/MMD1-related regulatory network required for completion of male and female gametogenesis, and possibly for sporogenesis, represent a heritage from ancestral land plants.

Introduction

The Plant HomeoDomain (PHD) motif defines a family of proteins that can recognise and bind histones depending on covalent modification status of the histone tails (Mouriz *et al.*, 2015). By recruitment and regulation of chromatin remodelling factors and transcriptional regulators, PHD proteins can thereby control chromatin compaction and gene expression in a histone modification-governed manner.

Phylogenetic analysis places angiosperm PHD proteins into five main clades and 16 subfamilies (Cao *et al.*, 2018). Among these, clade IIa comprises members from both mono- and dicotyledonous species including the Arabidopsis genes *MALE STERILITY 1* (*AtMS1*) and *MALE MEIOCYTE DEATH 1* (*AtMMD1*). *AtMS1* and *AtMMD1* encode similar protein products that are both essential for pollen production in anthers (Wilson *et al.*, 2001; Reddy *et al.*, 2003; Yang *et al.*, 2003). Still, the two genes exert their functions in distinct anther cell types. Therefore, *AtMMD1* controls gene expression and chromosome condensation needed for completion of meiosis in microsporocytes (Reddy *et al.*, 2003; Yang *et al.*, 2003) while *AtMS1* controls gene expression and function of tapetal cells surrounding and nursing the microsporocytes and microspores on their route towards functional pollen (Wilson *et al.*, 2001; Ito & Shinozaki, 2002; Alves-Ferreira *et al.*, 2007; Yang *et al.*, 2007; Reimegård *et al.*, 2017; Lu *et al.*, 2020). Both genes exert their functions through modification of chromatin structure.

Therefore, AtMS1 activates genes organised in clusters by the relaxation of chromatin condensation (Reimegård *et al.*, 2017) and AtMMD1 can bind histone tails in a modification-dependent manner (Andreuzza *et al.*, 2015; Wang *et al.*, 2016). A detailed mode of action was recently proposed for AtMMD1 in meiotic cells where the protein is recruited to H3K4me3 marks allowing it to modulate target specificity of nearby JUMONJI 16 (JMJ16) histone demethylases through a physical interaction dependent on its central MMD domain (Wang *et al.*, 2020).

The monophyletic group of land plants is characterised by a huge variation in reproductive solutions that is the result of successive key evolutionary innovations (Renzaglia *et al.*, 2000; Hackenberg & Twell, 2019; Hisanaga *et al.*, 2019; Rensing & Weijers, 2021; Sharma *et al.*, 2021). The developmental process controlled by *AtMS1* and *AtMMD1*, that is tapetum-assisted microspore and pollen formation facilitating downstream male gametogenesis, is for example a derived trait of angiosperms (Hackenberg & Twell, 2019). Gametogenesis in the common ancestors of all extant land plants is instead likely to have been reminiscent of that in bryophytes, ferns and lycophytes of today, where eggs and flagellated sperms are produced by female archegonia and male antheridia formed by a dominant haploid gametophyte generation (Renzaglia *et al.*, 2000; Hackenberg & Twell, 2019). These gametophytic reproductive organs were eventually lost from the angiosperm lineage as part of a drastic reduction of the haploid gametophyte generation accompanied by increased complexity of the diploid sporophyte generation

(Harrison, 2017). As part of this transition, pollen is hypothesised to have evolved from walled spores reminiscent of those in extant bryophytes thanks to two key evolutionary adaptations (Hackenberg & Twell, 2019). First, divisions in the male gametophyte generation were almost completely abolished to arrive at the situation in present-day angiosperms where only two sequential specialised divisions produce a pair of male gametes inside a vegetative cell from the primary meiotic product (the microspore). Second, breakage of the spore wall was deferred so that the cell divisions producing the two gametes could be completed within a still intact wall, today recognised as the angiosperm pollen wall. The proposed evolutionary origin of pollen indicates that tapetum-derived pollen production in angiosperms is related by descent to tapetum-dependent spore formation in bryophytes (Lopez-Obando et al., 2022).

The existence of PHD clade IIa homologues in gametophyte-dominant bryophytes (Higo et al., 2016; Sanchez-Vera et al., 2022), separated from angiosperms c. 450 million years ago (Ma) (Morris et al., 2018), suggests that clade IIa-related genes were present already in the common ancestors of all extant land plants. Recent transcriptome data from the bryophyte model moss Physcomitrium patens report the expression of two clade IIa homologues in sporophytes at stages during which tapetal-like cells are active and spores and their precursors develop (Perroud et al., 2018; Lopez-Obando et al., 2022). Moreover, the expression of the two genes was also detected in antheridia (male reproductive organs) and in the egg cell in archegonia (female reproductive organs), both produced by the haploid gametophytic generation (Meyberg et al., 2020; Sanchez-Vera et al., 2022 and references therein). Similarly, a putative clade IIa homologue of the model liverwort Marchantia polymorpha is also active in reproductive organs, at least in the antheridia (Higo et al., 2016). This points towards a function for bryophyte clade IIa genes during gametogenesis. Further dissection of this function may add to our understanding about the mechanisms, regulation and evolution of gametogenesis in land plants (Berger & Twell, 2011; Hisanaga et al., 2019).

Here we describe the functional characterisation of the clade IIa PHD homologues PpMS1A and PpMS1B in the moss P. patens. PpMS1A and PpMS1B are together required for male and female fertility by providing functions essential for the development of the gamete-producing inner cells of both antheridia and archegonia. The expression domains of the two genes furthermore suggest functions in sporogenous cells and in foot transfer cells of the diploid sporophyte generation. Based on these findings, we discuss a possible ancestral function for clade IIa PHD proteins and elaborate on how this may have evolved into the functions evident in present-day bryophytes and angiosperms.

Materials and Methods

Plant material, growth conditions, tissue harvest, transformation and crosses

Physcomitrium patens (previously Physcomitrella patens) ecotype Reute (R) (Hiss et al., 2017) was used as the wild-type (WT) and is the background to all transgenic lines in this study. Protonemal moss tissue was grown aseptically on solid BCD medium (Thelander et al., 2007) supplemented with 5 mM ammonium tartrate and 0.8% agar in Petri dishes at 25°C under constant white light from fluorescent tubes (F25T8/TL741; Philips, Amsterdam, the Netherlands) at 35 µmol m^{-2} s^{-1} in a Percival Scientific CU-41L4 growth chamber (Percival Scientific, Perry, IA, USA). To induce reproductive organs and subsequent sporophyte development, young chloronemal tissue was shaped into round balls and placed on solid BCD medium in 15 mm deep Petri dishes (90 mm in diameter). The ball-shaped tissue was allowed to grow out into gametophore-containing colonies for 5–6 wk after which the plates were transferred to SD conditions (8 h of light, 30 µmol m^{-2} s^{-1}) at 15°C in a Sanyo MLR-350 light chamber (Sanyo Electric, Tokyo, Japan) to induce reproductive development. To enhance fertilisation the plants were submerged in water overnight at 20 ± 1 dpi. Crosses were carried out as described in Thelander et al. (2019) and the P. patens ecotype Gransden was used as a WT line with strongly reduced male fertility. For expression and phenotype analysis, gametophyte shoots harbouring either reproductive organs or a developing sporophyte in the apex were harvested from the periphery of moss colonies at the indicated time points. Under a Leica MZ16 stereomicroscope (Leica Biosystems, Heidelberg, Germany), all leaves were removed to expose the antheridia and archegonia. For sporophyte analysis, also the residual reproductive organs were detached, as were the sporophyte calyptra from stage 8. To enhance the uptake of solutions for GUS staining, fixation, infiltration and historesin embedding, sporangia harvested after 12 dpw were punctuated using a fine needle. Protoplast transformation was carried out as previously described (Schaefer et al., 1991). Stable transformants were selected in the presence of 50 µg ml^{-1} hygromycin (H0192; Duchefa, Haarlem, the Netherlands) or G418 (11811023; Thermo Fisher Scientific, Waltham, MA, USA).

Generation of reporter lines

Primer sequences are shown in Supporting Information Table S1. The PpMS1A translational reporter construct pMLO14 (Fig. S1a), used to integrate a GFP-GUS gene in frame near the end of the coding sequence was generated by the fusion of four PCR fragments using In-Fusion technology (TaKaRa Bio): A 4550-bp vector fragment amplified with primers SS748/SS749 from plasmid pDEST14 (Thermo Fisher), a fragment covering 669 bp from exon 3 to near the end of the PpMS1A CDS amplified with primers SS750/SS751 from WT gDNA, a fragment covering a 2556-bp GFP-GUS gene amplified with primers SS752/SS753 from plasmid pMT211 (Thelander et al., 2019), and a fragment covering 651 bp of the extreme end of the CDS and the 3'UTR of PpMS1A amplified with primers SS754/SS755 from WT gDNA. To generate the PpMS1Apro::PpMS1A-GFPGUS reporter lines, 8 µg of pMLO14 and 4 µg of pMLO13 were co-transformed into WT protoplast together with 8 µg pACT1:hCAS9 and 4 µg of pBNRF (Schaefer et al., 2010; Lopez-Obando et al., 2016). Stable transformants were selected on G418, where after the in-frame fusion between the PpMS1A CDS and the GFP-GUS gene resulting from the correct

integration was confirmed by PCR amplification using the primers SS756/SS627, followed by sequencing of the resulting PCR product with the primers SS757 and SS627. Three independent lines showing correct integration were selected for downstream analysis (Table S2). If not stated otherwise, for each line, at least 10 specimens of each relevant stage and organ type were analysed for reporter signals with consistent results. The three lines indicated qualitatively similar signal patterns but, while signals in *PpMS1Apro::PpMS1A-GFPGUS-1* were strong and coherent in both reproductive organs and sporophytes, signals in *PpMS1Apro::PpMS1A-GFPGUS-2* and *-3* were generally weaker, and, as a consequence of this, challenging to detect in reproductive organs.

To produce the *PpMS1B* transcriptional reporter construct pVS1 (Fig. S1b), the *PpMS1B* promoter was amplified from gDNA with primers SS738/SS739, trimmed to 2918 bp with *Bam*HI/*Nco*I, and cloned between the same sites of the vector pMT211. The vector pMT211 carries a hygromycin selection cassette and allows promoters to be cloned ahead of a *GFP-GUS* reporter gene for subsequent integration into the *Pp108* locus (Thelander *et al.*, 2019). The resulting construct was verified by sequencing and linearised with *Sfi*I before transformation into WT plants. Correct integration was confirmed by PCR verification of 5′ and 3′ junctions with the primers SS5/SS742 and SS399/SS307, respectively (Fig. S1c,d). Three independent lines showing correct integration (*PpMS1B::GFPGUS-1,2,3*) were selected for downstream analysis. For each line, at least 10 specimens of each relevant stage and organ type were analysed for reporter signals with consistent results.

Generation of loss-of-function mutants

Primer sequences are shown in Table S1. *PpMS1A* loss-of-function mutants were generated by CRISPR technology, and gRNA-expressing constructs were designed using CRISPOR (Haeussler *et al.*, 2016). For each gRNA used, putative off-targets had at least four mismatches making off-target editing events highly unlikely (Table S3; Modrzejewski *et al.*, 2020). To produce the plasmids pMLO11 and pMLO12 (Table S3; Fig. S2a), AttB1-PpU6-SgRNAs-AttB2 fragments produced by gene synthesis (Integrated DNA Technologies, Coralville, IA, USA) were cloned into the vector pDONR221 by Gateway recombination (Invitrogen). To produce plasmid pMLO13 (Table S3; Fig. S2a), the annealing product of the complementary primers SS743/SS744 was cloned into vector pENTR_PpU6_L1L2 opened with *Bsa*I (Mallett *et al.*, 2019). Inserts were confirmed by sequencing. CRISPR mutants were then obtained as previously described (Lopez-Obando *et al.*, 2016). In short, WT or *ms1b-1* (please refer to subsequent paragraphs) protoplasts were co-transformed with 8 μg of pACT1:hCAS9, 4 μg of pBNRF, and 4 μg of each of the plasmids pMLO11 and pMLO12 or pMLO13. Transformants were selected in the presence of G418 and mutations were evaluated by PCR amplification and sequencing of gDNA with the gene-specific primers SS745/SS746 and SS745/SS747 (Table S2; Fig. S2a). For phenotypic analysis, three single (*ms1a-1,2,3*) and two double (*ms1ams1b-1,2*) mutant lines with mutations in *PpMS1A*, likely to block protein function, were

selected for phenotypic analysis (Table S2). For each line, a minimum of 20 specimens of each relevant stage and organ type were subjected to phenotypic analysis with consistent results.

PpMS1B loss-of-function mutants were generated by homologous recombination and, to produce the *PpMS1B* knockout construct pVS2 (Fig. S2b), Gateway 3-fragment recombination technology was used (Thermo Fisher). Therefore, LR recombination was used to fuse a 909-bp *PpMS1B* 5′ fragment (amplified with the primers SS734/SS735 and cloned into the entry vector pDONR P1-P4), a G418 resistance fragment from the entry clone pDONR4r-3r-G418 (Landberg *et al.*, 2020), and a 1180-bp *PpMS1B* 3′ fragment (amplified with the primers SS736/SS737 and cloned into the entry vector pDONR P3-P2), into the destination vector pDEST14. The resulting construct was verified by sequencing and was linearised with *Hpa*I/*Avr*I before transformation into WT moss and the selection of stable transformants in presence of hygromycin. Correct integration was confirmed by PCR verification of 5′ and 3′ junctions with the primers SS58/SS759 and SS762/SS763, respectively (Fig. S2c). Two independent lines showing the correct integration (*ms1b-1,2*) were selected for downstream analysis. For each line, a minimum of 20 specimen of each relevant stage and organ type was subjected to phenotypic analysis with consistent results.

RT-qPCR

For analysis of *PpMS1A* and *PpMS1B* expression in various WT tissues, samples from gametophore apices harvested at different time points after induction, antheridia, archegonia, and sporophyte samples corresponding to different developmental stages have been previously described (Landberg *et al.*, 2020; Lopez-Obando *et al.*, 2022). Tissue harvest, RNA extraction, cDNA synthesis and amplification, setup and cycling of qPCR reactions, normalisation using three reference genes, and calculations have been previously described (Landberg *et al.*, 2020). The gene-specific primers used were SS586/SS587 for *PpMS1A* and SS584/SS585 for *PpMS1B* (Table S1). To avoid amplification of genomic DNA contamination, the annealing site for one primer in each pair was interrupted by an intron. Melt curve, gel, and standard curve analyses confirmed that both primer pairs amplified a single product of the expected size with efficiencies close to 100% (data not shown). Data are presented as relative expression calculated using the $2^{-\Delta\Delta C_T}$ method. In Fig. 1(b,c) the sample with the highest transcript abundance for each gene was set to 1. In Fig. S3(a,b), the same data are presented, but here the sample with the highest overall transcript abundance (regardless of whether it was *PpMS1A* or *PpMS1B*) was set to 1. Each data point was based on biological triplicates and error bars represented standard deviations.

Sequence retrieval, proteins alignments and phylogenetic analysis

Gene and protein sequences of PHD clade IIa homologues displayed in the phylogenetic tree of Fig. 1(a) were retrieved following BLAST-based gene identification from phycocosm.jgi.doe.gov
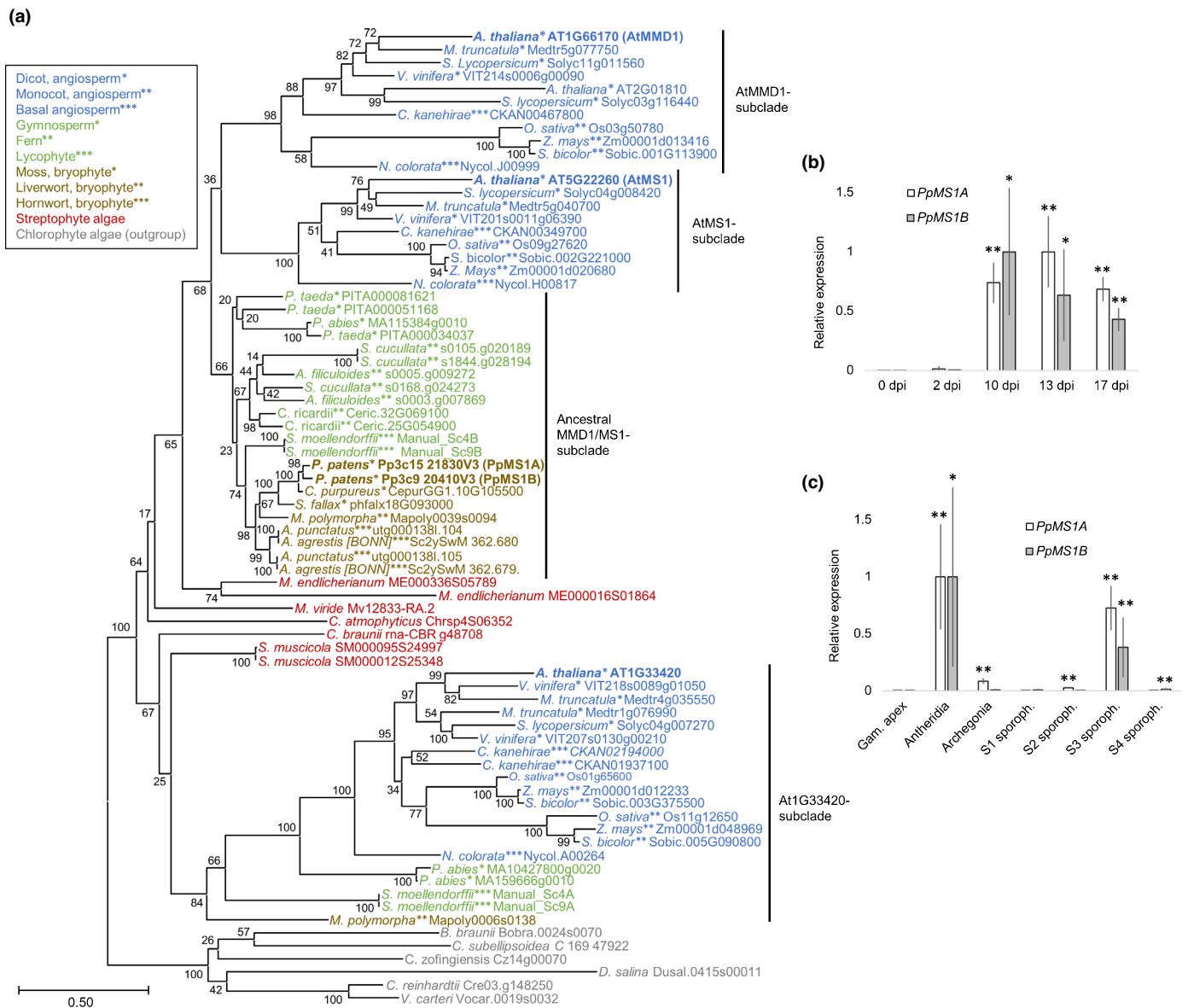
(a)

(b)

(c)

Fig. 1 Phylogeny of plant PHD clade IIa homologues and their expression in the moss *Physcomitrium patens*. (a) Maximum likelihood tree demonstrating the phylogenetic relationship of PHD clade IIa-related transcription factors from representative species of the main land plant lineages and from streptophytic algae, using homologues from chlorophytic algae as the outgroup. The taxonomic belonging of species represented in the tree is indicated by a combination of colour and number of asterisks according to the boxed key. (b) Relative transcript abundance of *PpMS1A* and *PpMS1B* in WT gametophore apices at different days post induction (dpi) of reproductive development. Typical occurrence of reproductive organs at selected time points: 0 and 2 dpi, no reproductive organs; 10 dpi, young antheridia; 13 dpi, mid-stage antheridia and young archegonia; 17 dpi, mature antheridia and mid-stage archegonia. (c) Relative transcript abundance of *PpMS1A* and *PpMS1B* in isolated WT gametophore shoot apices (without reproductive organs), antheridia bundles, archegonia bundles and sporophytes of different developmental stages. Sporophyte samples contain organs roughly correlating to the following stages described in Lopez-Obando *et al*. (2022): S1, st.1–3; S2, st.4–8; S3, st.9–11; S4, st.12–14. In both (b, c), the sample with the highest transcript abundance for each gene is set to 1, each data point represents an average of three independent biological replicates, error bars indicate standard deviation and asterisks indicate a statistically significant difference from gametophore apex sample before reproductive organ formation (Student's *t*-test: *, $P < 0.05$; **, $P < 0.01$). Please refer to also Supporting Information Fig. S3(a,b) for presentation of the same data in a way making comparisons of transcript abundance levels between *PpMS1A* and *PpMS1B* possible.

(streptophytic algae), hornworts.uzh.ch (hornworts), fernbase.org (ferns), congenie.org (gymnosperms), and PHYTOZOME v.13 (all other). Gene models for Solyc03g116440 from *Solanum lycopersicum*, Zm00001d020680 from *Zea mays*, and s1844.g028194 from *Salvinia cucullata* were subjected to minor manual curation. Gene models from four *Selaginella moellendorffii* loci were

manually assigned altogether. For phylogenetic reconstruction, amino acid sequences were aligned using the M-COFFEE algorithm in T-COFFEE (Notredame *et al*., 2000; Wallace *et al*., 2006) after which the alignment was filtered using Transitive Consistency Scores (Chang *et al*., 2014). The resulting filtered alignment (Fig. S4) was used for phylogenetic reconstruction in

MEGAX (v.10.1.5; Kumar *et al.*, 2018) with the maximum likelihood method (JTT amino acid substitution model, gamma distribution among sites) and 500 replications of bootstrapping. The nonfiltered alignment of full length proteins in Fig. S5 was also produced using the M-COFFEE algorithm in T-COFFEE. Alignments in Figs S4 and S5 were displayed using CLUSTALX 2.1 software (Larkin *et al.*, 2007).

GUS staining

Gametophore apices with reproductive organs or sporophytes were harvested as described above and incubated in GUS solution (50 mM $NaPO_4$, pH 7.2, 2 mM $Fe^{2+}CN$, 2 mM $Fe^{3+}CN$, 2 mM X-Gluc and 0.2% (v/v) Triton X-100) at room temperature for 48 h. For analysis of intact organs the tissue was transferred to 70% EtOH and, before analysis, the organs were mounted on objective glasses in 30% glycerol. For sectioning, the tissue was transferred from GUS solution to the FGPX fixative (Lopez-Obando *et al.*, 2022) and then treated as describe in the following section.

Sporophyte sectioning

Thin sectioning of sporophytes was carried out as described in Lopez-Obando *et al.* (2022). In short, samples were incubated overnight in FGPX fixative, dehydrated in an ethanol series, infiltrated twice in activated historesin solutions of different strengths, and embedded in activated historesin with hardener in plastic moulds. For phenotypic analyses, 6-μm longitudinal sections produced using a microtome equipped with a glass knife were dried-in onto microscopy slides and stained with toluidine blue. Sections of GUS-stained sporophytes were produced in the same way, but here sections were cut to be 10 μm thick and toluidine blue staining was omitted.

Microscopy

Intact GUS-stained reproductive organs and sporophytes mounted in 30% glycerol as well as toluidine blue- or GUS-stained sections of mutant and reporter lines were analysed using an Axioscope A1 microscope equipped with an AxioCam ICc 5 camera and the ZEN BLUE software (Zeiss) at ×10, ×20 and ×63 magnification. Images of mutant antheridia and archegonia mounted in 30% glycerol were captured using a DMI4000B microscope with differential interference contrast optics at ×63 magnification, a DFC360FX camera, and LAS AF software (Leica Microsystems, Wetzlar, Germany). For GFP expression analysis, reproductive organs and the developing sporophytes of the indicated reporter lines were harvested and mounted in water immediately before analysis. Signals were documented using a LSM 780 confocal laser scanning microscope (Carl Zeiss) with a GaAsP detector and ×20 (NA 0.8) and ×63 (NA1.2, water immersion) objectives. Excitation/detection parameters were 488 nm/491–598 nm for GFP and 633/647–721 nm for chlorophyll autofluorescence. Images were acquired using ZEN BLACK software and are snapshots of a single focal plane with selected

channels overlaid. Adobe PHOTOSHOP CC was used to adjust intensity and contrast, mark borders and cells, cut away surrounding areas and merge images to visualise entire large organs at high magnification. Bar charts, tables, calculation of means, standard deviation and Student's *t*-test were performed using Microsoft EXCEL.

Results

PHD clade IIa transcription factors predate the emergence of land plants

Previous phylogenetic analyses places the Arabidopsis genes *AtMS1*, *AtMMD1*, *AT2G01810*, and *AT1G33420* in subfamily IIa of PHD transcription factors (Cao *et al.*, 2018). To confirm the suggested existence of subfamily IIa PHD genes also in bryophytes (Higo *et al.*, 2016; Sanchez-Vera *et al.*, 2022), we screened green plant genomes for homologues. This revealed subfamily IIa PHD genes not only in all major land plant lineages, but also in their streptophytic algal sisters and in chlorophytic algae. Deduced amino acid sequences were subjected to phylogenetic analyses using chlorophyte sequences as an outgroup (Figs 1a, S4). The resulting tree places land plant sequences in four well supported subclades: The angiosperm-specific MMD1 and MS1 subclades; an ancestral MS1/MMD1 subclade gathering the majority of bryophyte, lycophyte, fern, and gymnosperm sequences; and the At1G33420-subclade harbouring sequences primarily from angiosperms but also from gymnosperms, ferns and a liverwort (Fig. 1a). The relationships of these four distinct subclades are more poorly resolved, but the tree indicates that the angiosperm-specific MS1 and MMD1 subclades emerged from within the ancestral MS1/MMD1 subclade via a duplication event taking place in the common ancestor of monocots and dicots. A common origin for land plant genes belonging to the MMD1, MS1, and ancestral MMD1/MS1 subclades is further supported by identical intron positioning and the conservation of domains in their protein products demonstrated to be functionally important in angiosperm MS1 and/or MMD1 proteins (Fig. S5). Therefore, well conserved regions include the C-terminal PHD domain, a suggested N-terminal nuclear localisation signal, and the internal MMD domain that in AtMMD1 regulates the substrate specificity of the JMJ16 histone demethylase by a physical interaction (Fig. S5; Wilson *et al.*, 2001; Ito & Shinozaki, 2002; Reddy *et al.*, 2003; Yang *et al.*, 2003; Wang *et al.*, 2020).

PpMS1A and *PpMS1B* are expressed in developing sporophytes, as well as in male and female reproductive organs

To reveal the function of PHD clade IIa genes in bryophytes, and with hope of gaining insight about ancestral functions of this gene family in land plants, we have functionally characterised the two *P. patens* subfamily IIa homologues *PpMS1A* (Pp3c15_21830V3.1) and *PpMS1B* (Pp3c9_20410V3.1). As published transcriptome data indicate that *PpMS1A* and *PpMS1B* are exclusively expressed in the early sporophyte

generation, and in reproductive organs produced by the haploid gametophyte generation (Sanchez-Vera *et al.*, 2022 and references therein), we first verified this using qPCR. We checked the expression in gametophore (gametophytic shoot) apices at different times post induction (dpi) of reproductive development (for typical ontogeny, please refer to Landberg *et al.*, 2013). This revealed a complete lack of expression in apices yet to develop reproductive organs (0, 2 dpi), but a clear expression of both genes in apices that had developed reproductive organs (10, 13, 17 dpi) (Figs 1b, S3a). Next, we checked expression in isolated antheridia and archegonia, as well as in isolated sporophytes of different developmental stages. This revealed significantly increased expression in all three tissue types of at least one of the genes when compared with vegetative shoot apices (Figs 1c, S3b). Antheridia showed highly significant expression of both genes, whereas expression in archegonia was lower and proved significant only for *PpMS1A*. The relatively low expression in archegonia may be explained by expression in only a fraction of the cells in the organ, a prospect fitting well with the previous observation that expression of the two genes is scored in eggs but not in cavity wall cells (Sanchez-Vera *et al.*, 2022). In sporophytes, transcript abundance of both *PpMS1A* and *PpMS1B* peaked in the S3 sample (Ortiz-Ramirez *et al.*, 2016), corresponding to developmental stages 9–11 in Lopez-Obando *et al.* (2022), indicating active expression sometime between completion of embryogenesis and the appearance of mature spores. Finally, even if comparisons of expression between genes based on qPCR data should be handled with care, our data indicate that *PpMS1A* is expressed at generally higher levels than *PpMS1B* (Fig. S3a,b).

PpMS1 activity is essential for developmental progression of spermatogenous cells

In the haploid gametophyte generation, all three major lineages of bryophytes produce flagellated sperms in antheridia (Renzaglia *et al.*, 2000). In *P. patens*, the vegetative shoot apex is reprogrammed to produce antheridia in response to low temperatures and short day-length through a stereotypical developmental programme (Hohe *et al.*, 2002; Landberg *et al.*, 2013; Hiss *et al.*, 2017; Kofuji *et al.*, 2018). To get a more detailed picture of where and when during antheridia development the *PpMS1* genes are expressed, we produced translational reporter lines for *PpMS1A* (*PpMS1Apro::PpMS1A-GFPGUS-1,2,3*) and transcriptional reporter lines for *PpMS1B* (*PpMS1Bpro::GFPGUS-1,2,3*) (the Materials and Methods section; Fig. S1).

The translational *PpMS1A* reporter showed signals in antheridial inner cells from stages 3–7, with a peak around stage 5, whereas no signals were detected in jacket and tip cells (Fig. 2a; stages defined in Landberg *et al.*, 2013). PpMS1A expression was therefore restricted to the spermatogenous cells, and occurs as soon as they appear, stays active throughout their division phase, and fades out at around their entrance into spermatogenesis. By contrast, the transcriptional *PpMS1B* reporter failed to detect expression in any stage or in any part of the antheridia. This fits well with our qPCR data indicating a significant but several fold lower expression of *PpMS1B* than of *PpMS1A* in antheridia (Fig. S3a,b).

To address the functional relevance of *PpMS1* expression in antheridia, we went on to produce single and double loss-of-function mutants for the two genes. *PpMS1A* single mutants (*ms1a-1,2,3*) were produced by CRISPR editing, *PpMS1B* single mutants (*ms1b-1,2*) were produced by homologous recombination, and double mutants (*ms1ams1b-1,2*) were produced by CRISPR editing of *PpMS1A* on the *ms1b-1* background (the Materials and Methods section; Fig. S2). Although neither single loss-of-function mutant showed obvious deviations in antheridia development, the male organs of *ms1ams1b* double mutants displayed an arrest of inner cell development resulting in a complete inability to produce functional sperms (Fig. 2b,c). The periclinal divisions in the early antheridium giving rise to the first 4–6 inner cells appeared unaffected, and the newly formed inner cells typically also divided once but, after this, inner cell divisions ceased in the double mutant. WT inner cells continued to divide at the expense of cell size during stages 4–6, after which they entered spermatogenesis at stage 7, but double mutant inner cells instead remained large and kept an appearance similar to the outer cells from which they had first originated (Fig. 2b,c; Table S4). The sterile jacket and tip cells of double mutant antheridia matured as in WT, as indicated by their elongation/pigmentation and swelling/vacuolation, respectively, even if the organ tip failed to open at maturity. This suggests that jacket and tip cell maturation is independent on successful differentiation of inner cells into sperms, but that the bursting of organ tips may somehow require the formation of sperms.

PpMS1 activity is needed for canal clearance and egg cell maturation in archegonia

Physcomitrium patens female reproductive organs (archegonia) are initiated from a lateral position close to the gametophore apex a few days after the outgrowth of the first antheridia, and their development has been described previously (Kofuji *et al.*, 2009; Landberg *et al.*, 2013, 2020). Signals in archegonia from the translational *PpMS1A* reporter were restricted to the central cell file, consisting of a basal-most pre-egg/egg, an upper basal cell, and four canal cells (two basal and two apical) (Fig. 3a). The signals indicated relatively strong PpMS1A protein expression in the pre-egg/egg and the upper basal cell from stages 5 to 7, after which expression in these two cells declined successively during stages 8 and 9, when the egg matures and the canal cells degrade (stages defined in Landberg *et al.*, 2013). The reporter also indicated weak PpMS1A expression in canal cells from stages 6 to 8. As in antheridia, we were unable to detect signals from the transcriptional *PpMS1B* reporter in archegonia, probably reflecting generally low expression levels as indicated by our initial qPCR experiments (Figs 1c, S3d).

The phenotypic defects of the *ms1ams1b* archegonia correlated spatially and temporally with the expression domains of the *PpMS1A* reporter (Fig. 3b). Archegonia from the *ms1ams1b* double mutant developed normally until stage 7, by concluding cell divisions in the central cell file including an asymmetric division of the basal-most cell to produce the egg and the upper basal cell. However, they consistently failed to complete degradation of the
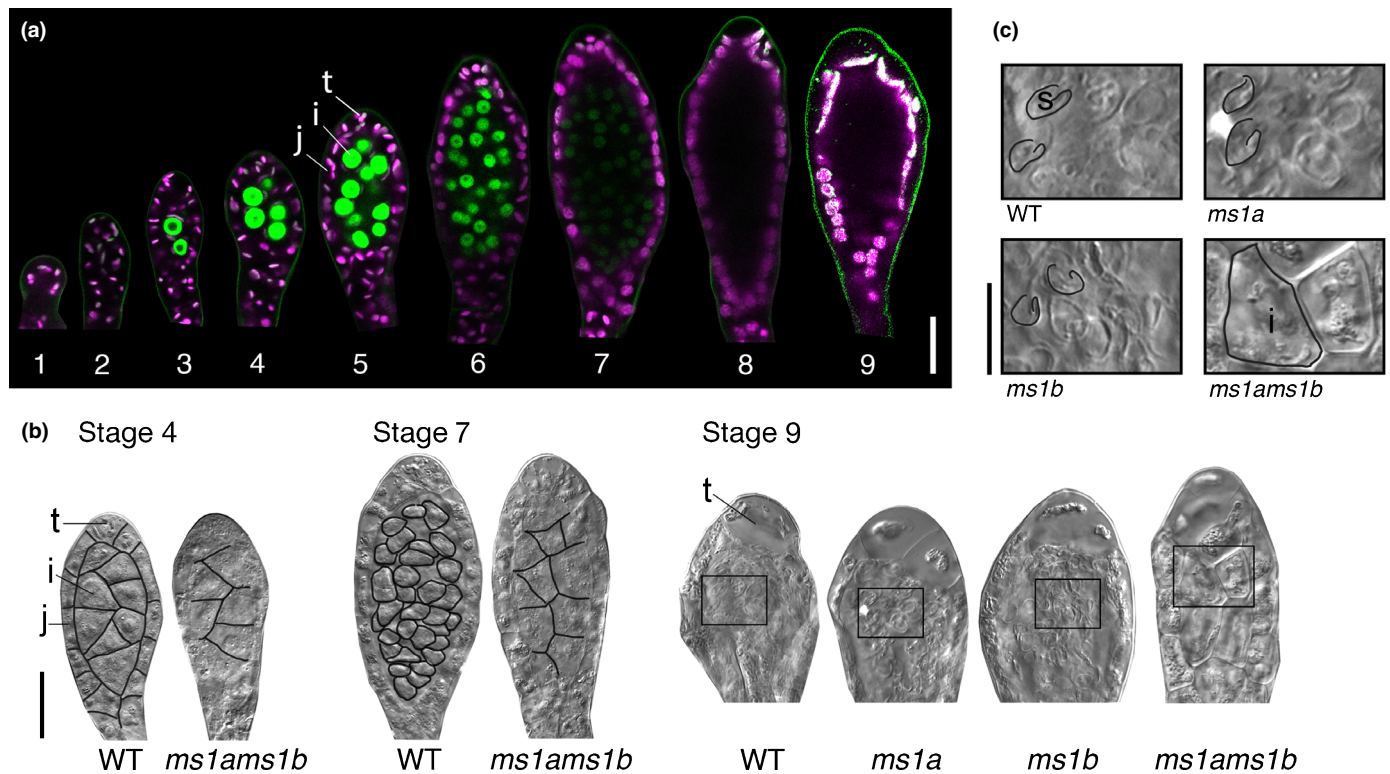
Fig. 2 *PpMS1* functions in *Physcomitrium patens* antheridia. (a) *PpMS1A::PpMS1A-GFPGUS-1* reporter signals in representative antheridia. A merge of confocal channels detecting green fluorescent protein (green) and chloroplast autofluorescence (magenta) is shown, and the numbers 1–9 indicate developmental stages according to Landberg *et al.* (2013). Each image shows a medial focal plane through an organ with radial symmetry in which all cell types can be seen. Note the expression in spermatogenous inner cells from stages 3 to 7. Bar, 20 μm. (b) Differential interference contrast images of representative stages 4, 7 and 9 antheridia from wild-type (WT) and the *ms1ams1b-1* double mutant. Note problems with proliferation and differentiation of spermatogenous inner cells in the double mutant. Stage 9 *ms1a-1* and *ms1b-1* single mutant antheridia are also shown to demonstrate normal sperm production in these genotypes. Bar, 20 μm. (c) High magnification of boxed areas in stage 9 organs in (b). Bar, 10 μm. Cell type labels: tip cells (t); jacket cells (j); inner cells (i); sperm cells (s). In (b, c), contours of selected cells have been marked in black for clarity.

upper basal cell and canal cells during stage 8, which is required for the formation of an open canal down to the egg through which sperms can enter when the organ tip opens at stage 9 (Fig. 3b; Table S5). This deficiency prevented canal clearance, and is likely to block sperm access to the egg, even if the organ tip opened as in WT during stage 9. We also observed that egg cells in stage 9 *ms1ams1b* archegonia were generally smaller and more compact than in WT (Fig. 3b; Table S5).

While the *ms1b* single mutant produced WT-like archegonia, the female reproductive organs of the *ms1a* single mutant showed similar but milder deficiencies compared with *ms1ams1b* organs, with only partially blocked degradation of upper basal and canal cells, and lower penetrance of abnormal egg cell compaction (Fig. 3b; Table S5). The fact that phenotypes in the *ms1ams1b* double mutant were more severe than in the *ms1a* single mutant suggests that *PpMS1B* contributed to *PpMS1* functions in archegonia, at least in the absence of *PpMS1A*.

PpMS1 functions are essential for both male and female fertility

Physcomitrium patens is a monoicous species fully capable of self-fertilisation (Perroud *et al.*, 2019). To assess the effect of reduced

or lost *PpMS1* function on fertility, we next carried out a series of crossing experiments. The results confirmed that the *ms1ams1b* double mutant is completely unable to self (Table 1). This was expected as the double mutant cannot produce sperms (please refer to above), but crosses also showed that sporophyte production from mutant archegonia could not be restored even when the highly fertile Reute WT was used as the sperm donor, indicating that the double mutant was both male and female sterile (Table 1).

We also explored the fertility of the *ms1a* single mutant by subjecting it to selfing and crosses to both the fertile Reute WT and the largely male sterile Gransden WT (Landberg *et al.*, 2020; Meyberg *et al.*, 2020). The crosses showed that the *ms1a* single mutant can self, albeit at much lower frequencies than its parental Reute WT, indicating that the single mutant suffers from reduced fertility but is able to produce fertilisation competent male and female gametes to some extent (Table 1). The much-reduced fertilisation frequency could not be restored, even when the highly fertile Reute WT was used as the sperm donor, indicating that the deficiency was mainly due to a female fertility problem (Table 1). This conclusion was partially supported by the ability of *ms1a* single mutant sperms to significantly increase the frequency of sporophyte formation from archegonia of the
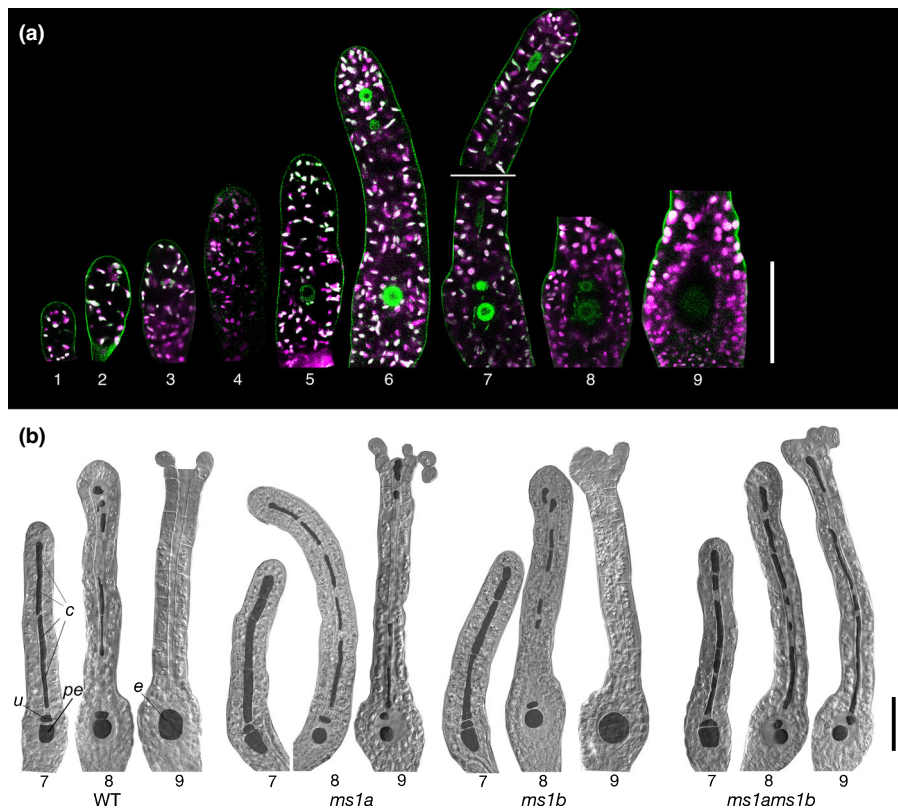
Fig. 3 *PpMS1* functions in *Physcomitrium patens* archegonia. (a) *PpMS1A::PpMS1A-GFPGUS-1* reporter signals in representative archegonia. A merge of confocal channels detecting green fluorescent protein (green) and chloroplast autofluorescence (magenta) are shown, and the numbers 1–9 indicate developmental stages according to Landberg *et al.* (2013). Each image represents a single near-medial plane from a full Z-stack of an organ representative for that stage. Cells in planes or parts of organs not shown produced no signals. The white line in the stage 7 organ indicates that basal and apical portions are from different Z-planes. Note the expression in the central file of inner cells. Bar, 50 μm. (b) Differential interference contrast images of representative stages 7, 8 and 9 archegonia from wild-type (WT) and the *ms1ams1b-1* double mutant. Note the problems with degradation of upper basal cell and canals cells during stages 8 and 9, and the reduced size of the egg at stage 9 in the double mutant. Stages 8 and 9 *ms1a-1* organs, displaying a mild version of the double mutant phenotype, and stage 9 *ms1b-1* single mutant archegonia, displaying no clear phenotype, are also shown. Please refer to Supporting Information Table S5 for numerical data. Inner cells have been false coloured in dark grey for clarity. Cell type labels: canal cells (c); upper basal cell (u); pre-egg (pe); egg (e). Bar, 50 μm.

Table 1 Fertility of *Physcomitrium patens ms1* mutants.

Female genotype	Male genotype	Number of shoots analysed	Frequency of shoots with initiated sporophyte development (%)
R WT	R WT	300	98
Gd WT	Gd WT	448	0.9
Gd WT	R WT	48	71
ms1b-1	*ms1b-1*	284	95
ms1a-2	*ms1a-2*	233	0.9
Gd WT	*ms1a-2*	148	32
ms1a-2	R WT	248	1.2
ms1a-3	*ms1a-3*	232	1.3
ms1ams1b-1	*ms1ams1b-1*	456	0
ms1ams1b-2	*ms1ams1b-2*	357	0
ms1ams1b-2	R WT	387	0

Number of shoots that formed sporophytes after selfing or after crosses between indicated *ms1* mutant line and wild-type (WT) strains Reute (R) or Gransden (Gd).

largely male sterile Gransden WT, demonstrating that *ms1a* single mutant sperms are at least partly functional (Table 1). As expected from its lack of reproductive organ phenotypes, the *ms1b* single mutant could self at a frequency similar to that of the WT.

PpMS1 expression domains suggests functions in the foot and in sporogenous cells of the sporophyte

PpMS1A and *PpMS1B* are also active in mid-stage sporophytes supporting a *PpMS1* function in the diploid generation (Figs 1d, S3b). As in all bryophytes, the moss zygote develops into a non-branched sporophyte consisting of a foot and an apical capsule (sporangium) in which sporogenous cells undergo meiosis to form spores. *Physcomitrium patens* sporophyte ontogeny is highly reproducible (Sakakibara *et al.*, 2008; Kofuji *et al.*, 2009; Daku *et al.*, 2016; Ortiz-Ramirez *et al.*, 2016; Yip *et al.*, 2016; Coudert *et al.*, 2019). For a definition of the developmental stages referred to below, please refer to Lopez-Obando *et al.* (2022).

Unfortunately, the PpMS1 loss-of-function mutants failed to provide clues to the functional relevance of *PpMS1* expression in sporophytes. As already described, the *ms1ams1b* double mutant was completely unable to produce sporophytes due to reproductive organ and gamete deficiencies (Figs 2, 3; Table 1), while the two single mutants produced WT-like sporophytes (albeit at reduced rates in the *ms1a* mutant) (Fig. 4a). This suggests that the two *PpMS1* genes have redundant functions during sporophyte development, a prospect supported by the fact that expression of the two genes peaks in S3 sporophytes and is less different in strength than in reproductive organs (Figs 1d, S3b). In addition, the reporter lines also revealed a spatial overlap of *PpMS1A* and *PpMS1B* expression in two discrete domains during sporophyte development. Although no signals were detected in young embryos, both reporters were actively expressed in the foot of the slender embryo with an onset at around stage 5 (Figs 4b, S6). The signals were largely concentrated to the epidermal transfer cells suggested to be important for nutrient uptake from the gametophore (Regmi & Gaxiola, 2017). Signals from the translational *PpMS1A* reporter eventually spread from the foot to parts of the seta connecting the foot to the sporangium, and largely persisted until sporophyte maturity. By contrast, signals from the transcriptional *PpMS1B* reporter were more restricted to the sporophyte foot and peaked in strength at around stage 8 after which they faded out.

In addition to expression in the sporophyte foot, the two reporters also indicated expression of *PpMS1A* and *PpMS1B* in the sporogenous cells. Therefore, signals from both reporters were evident in the sole sporogenous cell layer from early stage 9, that is immediately following completion of the cell division phase giving rise to the different cell layers of the sporangium (Figs 4b–d, S6). The signals in the sporogenous cells persisted during their final division at stage 10 and their maturation into liberated globular sporocytes at stage 11, after which the signals started to fade before meiosis and spore formation at stage 12 (Figs 4c,d, S6). Signals from the translational *PpMS1A* reporter peaked at stages 9 and 10 and were completely lost around meiosis at stage 12 (Fig. 4c,d). Signals from the transcriptional *PpMS1B* reporter peaked at stages 10 and 11, dropped in intensity at around meiosis at stage 12, but were often weakly evident as late as in mature spores (Figs 4c,d, S6).

Discussion

This study revealed that the PHD clade IIa genes in moss control developmental processes in antheridia, archegonia and possibly in sporophytes. *PpMS1* activity is absolutely essential both for male and female fertility, and fundamental features of how it affects the development of antheridia and archegonia are shared. *PpMS1* activity therefore appears to be dispensable for the initiation of the two organ types, the development of their sterile structural parts, and the inwards formative divisions giving rise to the gamete-producing inner cell population. Instead, *PpMS1* activity is needed for the specification and further development of these inner cells. In antheridia, *PpMS1* controls the proliferation and differentiation of inner cells into sperms. In archegonia, *PpMS1*

is needed for proper maturation of the egg, and for degradation of the remaining inner cells to leave a free canal passage for sperms to access the egg.

The reporter genes indicate that *PpMS1A* and *PpMS1B* have functions also in the diploid sporophyte generation. Their expression domains suggests that *PpMS1* activity is dispensable for early embryo development, but may have functions in transfer cells of the sporophyte foot and in the developing sporangium. In the sporangium, the *PpMS1* genes are expressed in the sporogenous cell layer soon after its establishment, supporting a possible function of *PpMS1* activity for the specification of these cells. In angiosperms, MS1 and MMD1 are part of a complex gene regulatory network facilitating tapetum-mediated pollen development (Ferguson *et al.*, 2017; Lei & Liu, 2020). Among other factors, this network also includes bHLH clade II and III(a+c) genes. The PpMS1 expression pattern in moss sporophytes, combined with that of PpbHLH clade II and III(a+c) genes (Lopez-Obando *et al.*, 2022), supported the fact that moss sporogenesis could be regulated by a homologous network inherited from the common ancestor of land plants.

Our finding that *PpMS1A* and *PpMS1B* provide possible functions in sporophytes, as well as during male and female gametogenesis, whereas the function of their angiosperm homologues is restricted to processes finally leading to completion of male gametogenesis only, raises questions about what may have been the original PHD clade IIa function in the ancestors of all extant land plants. We speculate that the functions in antheridia, archegonia, and possibly sporophytes of mosses today, all may have originated from the one and the same function in a hypothetical ancestral plant, with morphologically similar gametes (isogamy) and a haplontic life cycle in which the zygote underwent meiosis without intervening mitotic divisions. Therefore, we hypothesise that PHD clade IIa activity served to specify the two gametes, after which it was carried over via fertilisation to the zygote, in which it secured expression of genes needed, not only for meiosis, but also for nutrient uptake from the gametophyte generation, representing a feature hypothesised to have been pre-adaptive and critical for the emergence of multicellular sporophytes (Graham & Wilcox, 2000). Later during evolution, when mitotic divisions of the zygote morphologically separated the cells destined for meiosis from the cells carrying over nutrients from the gametophyte, this was accompanied by a similar spatiotemporal separation of clade IIa activity.

To challenge this speculative hypothesis, it would be highly interesting to investigate the expression pattern and function of possible PHD clade IIa homologues in the algal sisters of land plants (Fig. 1a; Ito *et al.*, 2007). Using a recent transcriptome study (Sanchez-Vera *et al.*, 2022), we in fact identified 135 additional moss genes with significantly higher expression levels in egg cells, antheridia and the diploid sporophyte generation at the green stage when sporogenesis occurs, compared with vegetative haploid tissues (Table S6). They therefore have the potential to play specific roles in both gametogenesis and sporogenesis. Possibly, the hypothetical evolutionary history outlined for clade IIa genes could be shared also with these genes. These include the two *PpBNB* genes encoding class VIIIa bHLH transcription
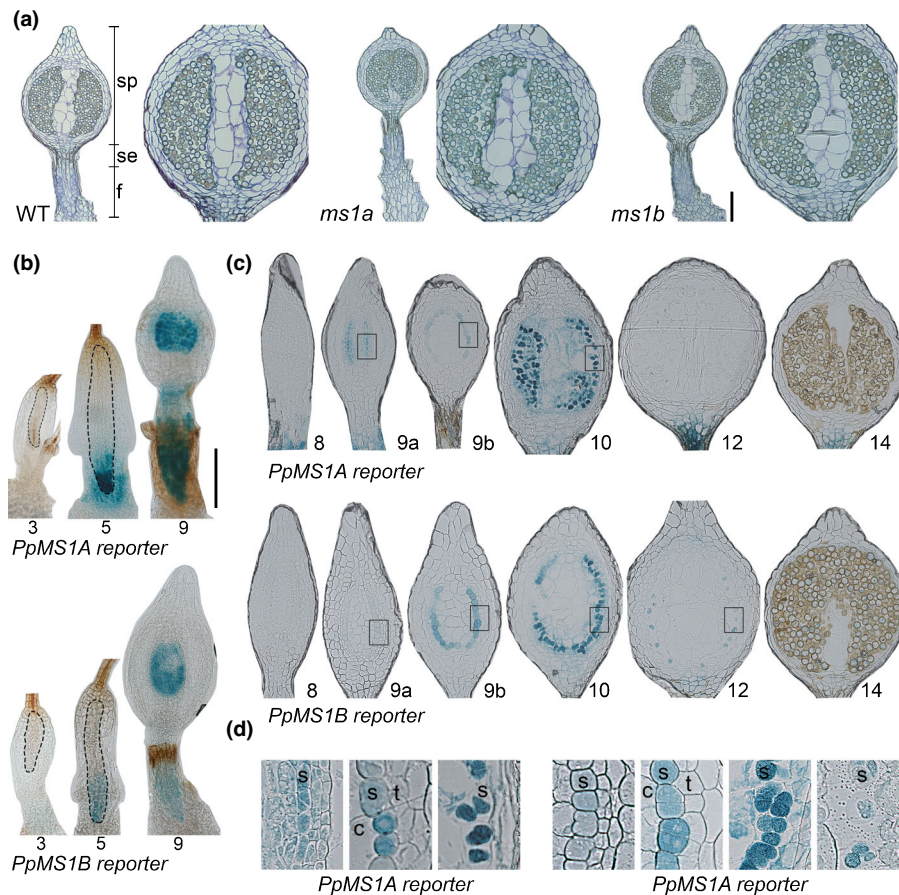
Fig. 4 *PpMS1* activity in *Physcomitrium patens* sporophytes. (a) Medial longitudinal sections through wild-type (WT), *ms1a-2* and *ms1b-1* stage 14 sporophytes to demonstrate the lack of phenotypes in *ms1* single mutants. For each genotype, an entire sporophyte is shown to the left and a magnification of a sporangium to the right. There is no size difference between the genotypes even if the *ms1a* sporophyte overview may give this impression, as the section is not perfectly medial through the sporangium. Labels: foot (f); seta (se); sporangium (sp). (b–d) *PpMS1A::PpMS1A-GFPGUS-1* and *PpMS1B::GFPGUS-1* GUS reporter signals in sporophytes. (b) Whole-mounted stages 3, 5–6 and 9 GUS-stained sporophytes of the *PpMS1A::PpMS1A-GFPGUS-1* (upper) and the *PpMS1B::GFPGUS-1* (lower) reporter lines. Note early signals in sporophyte foot and later signals in the central part of sporangium. Contours of stages 3 and 5 embryos have been traced with dashed lines for clarity. (c) Sections of stages 8, 9, 10, 12 and 14 GUS-stained sporangia of the *PpMS1A::PpMS1A-GFPGUS-1* (upper) and the *PpMS1B::GFPGUS-1* (lower) reporter lines. Some displayed sporangia were sectioned at an angle why organ tips are missing. Note that signals restricted to the sporogenous cell layer comes on at stage 9. (d) High magnification of boxed areas in (c) showing that *PpMS1A::PpMS1A-GFPGUS-1* (left) and *PpMS1B::GFPGUS-1* (right) signals are restricted to the sporogenous cell layer (s), whereas signals are missing from the surrounding columella (c) and tapetum (t) cells layers. Numbers in (b, c), indicate the developmental stages according to Lopez-Obando *et al.* (2022). Please refer also to Supporting Information Fig. S6 for *PpMS1B::GFPGUS-1* GFP reporter signals in sporophytes. Bars: (a–c) 200 µm; (d) 50 µm.

factors. Whereas the Arabidopsis *BNB* genes are required only for specification of male generative cells, the *M. polymorpha* homologues are essential for the initiation of both male and female reproductive organs, and are active in egg and sperm progenitors (Yamaoka *et al.*, 2018; Hisanaga *et al.*, 2019). In *P. patens*, *BNB*'s are important for both male and female germ cell specifications, making it difficult to assess their potential role in the green sporophyte, where it is also expressed (Sanchez-Vera *et al.*, 2022). A moss gene, *PpMKN1*, encoding a class 2 KNOTTED1-LIKE HOMEOBOX (KNOX2) transcription factor preventing haploid-specific development in the sporophyte phase (Sakakibara *et al.*, 2013) is also significantly upregulated in the egg and antheridia, although at a much-reduced level compared with the green sporophyte. Additional transcription factor genes, such as homologues to Arabidopsis *WRI2*, *LEC2*, *EFM*, *NAC56*, are also upregulated in all three reproductive tissue types, but their

functions in moss are unknown and not easy to extrapolate from their functions in Arabidopsis. A homologue to CCR4-NOT complex component NOT1, which in Arabidopsis regulates RNA-directed methylation and transcriptional silencing (Zhou *et al.*, 2020), is also elevated in the reproductive organs and the green sporophytes. AtNOT1 is necessary for example proper male germ cell development, pollen germination and embryogenesis (Motomura *et al.*, 2020; Pereira *et al.*, 2020). A moss homologue of MBD9, a SWR1-C interacting protein required for H2A.Z deposition at a subset of actively transcribing genes in Arabidopsis (Potok *et al.*, 2019; Luo *et al.*, 2020), also showed elevated expression in the three selected tissue types.

Assuming that the need for PHD clade IIa functions in moss to complete male and female gametogenesis and possibly sporogenesis represents a heritage from ancestral land plants, one can ask how this has evolved into the clade IIa regulation in anthers

evident in angiosperms. It appears very likely that this can be attributed to the loss of gametangia as part of a dramatic reduction of the gametophyte generation in angiosperms (Hisanaga *et al.*, 2019). Therefore, the need for clade IIa functions during gametogenesis may either have been lost, or at least become difficult to separate from sporophytic functions facilitating meiosis, as the two processes have become intimately coupled in time and space in angiosperms.

The possible homology between clade IIa functions in angiosperm anthers and moss sporangia is complicated by the fact that Arabidopsis *AtMS1* and *AtMMD1* exert their functions in distinct anther cell types. Therefore, *AtMMD1* controls gene expression and chromosome condensation in microsporocytes (Reddy *et al.*, 2003; Yang *et al.*, 2003), whereas *AtMS1* controls gene expression in tapetal cells (Wilson *et al.*, 2001; Ito & Shinozaki, 2002; Alves-Ferreira *et al.*, 2007; Yang *et al.*, 2007; Reimegård *et al.*, 2017; Lu *et al.*, 2020). Our phylogenetic analysis suggests that the occurrence in moss of a single type of the *MS1/MMD1* homologue may reflect an ancestral state, whereas the angiosperm-specific *MS1* and *MMD1* subclades emerged via a duplication event taking place in the common ancestor of monocots and dicots. If so, the distinct functions of *AtMS1* and *AtMMD1* may have evolved by neo- or subfunctionalisation from a function similar to that performed by *PpMS1* in extant moss sporangia.

Even if the current study does not address the molecular basis of *PpMS1* activity, the conservation of key protein domains, such as the N-terminal nuclear localisation signal, the central MMD domain, and the C-terminal PHD domain supports the idea that also bryophyte PHD clade IIa proteins function by controlling cell identity through the regulation of chromatin structure and gene expression (Andreuzza *et al.*, 2015; Reimegård *et al.*, 2017; Wang *et al.*, 2020). Future studies will aim to reveal if this is indeed the case, and to what extent related genes and gene clusters are targeted by clade IIa regulation in the angiosperm anther and in the reproductive organs and the sporophyte of moss.

Acknowledgements

Author contributions

KL, ML-O, VSV and MT conducted the experimental work and analysed the data. ML-O, KL, ES and MT designed experiments and interpreted data. MT, ES and KL wrote the manuscript.

ORCID

Katarina Landberg https://orcid.org/0000-0002-2945-8571
Mauricio Lopez-Obando https://orcid.org/0000-0002-1380-0643
Victoria Sanchez Vera https://orcid.org/0000-0001-8615-5270
Eva Sundberg https://orcid.org/0000-0003-4228-434X
Mattias Thelander https://orcid.org/0000-0002-6663-7405

Data availability

The data that support the findings of this study are available from the corresponding author upon request.

References

Alves-Ferreira M, Wellmer F, Banhara A, Kumar V, Riechmann JL, Meyerowitz EM. 2007. Global expression profiling applied to the analysis of Arabidopsis stamen development. *Plant Physiology* **145**: 747–762.

Andreuzza S, Nishal B, Singh A, Siddiqi I. 2015. The chromatin protein DUET/MMD1 controls expression of the meiotic gene TDM1 during male meiosis in Arabidopsis. *PLoS Genetics* **11**: e1005396.

Berger F, Twell D. 2011. Germline specification and function in plants. *Annual Review of Plant Biology* **62**: 461–484.

Cao Y, Han Y, Meng D, Abdullah M, Li D, Jin Q, Lin Y, Cai Y. 2018. Systematic analysis and comparison of the PHD-finger gene family in Chinese pear (*Pyrus bretschneideri*) and its role in fruit development. *Functional & Integrative Genomics* **18**: 519–531.

Chang J-M, Di Tommaso P, Notredame C. 2014. TCS: a new multiple sequence alignment reliability measure to estimate alignment accuracy and improve phylogenetic tree reconstruction. *Molecular Biology and Evolution* **31**: 1625–1637.

Coudert Y, Novak O, Harrison CJ. 2019. A KNOX-cytokinin regulatory module predates the origin of indeterminate vascular plants. *Current Biology* **29**: 2743–2750.

Daku RM, Rabbi F, Buttigieg J, Coulson IM, Horne D, Martens G, Ashton MW, Suh D-Y. 2016. PpASCL, the *Physcomitrella patens* anther-specific chalcone synthase-like enzyme implicated in sporopollenin biosynthesis, is needed for integrity of the moss spore wall and spore viability. *PLoS ONE* **11**: e0146817.

Ferguson AC, Pearce S, Band LR, Yang C, Ferjentsikova I, King J, Yuan Z, Zhang D, Wilson ZA. 2017. Biphasic regulation of the transcription factor ABORTEDMICROSPORES (AMS) is essential for tapetum and pollen development in Arabidopsis. *New Phytologist* **213**: 778–790.

Graham LKE, Wilcox LW. 2000. The origin of alternation of generations in land plants: a focus on matrotrophy and hexose transport. *Philosophical Transactions of the Royal Society of London. Series B: Biological Sciences* **355**: 757–767.

Hackenberg D, Twell D. 2019. The evolution and patterning of male gametophyte development. *Current Topics in Developmental Biology* **131**: 257–298.

Haeussler M, Schönig K, Eckert H, Eschstruth A, Mianné J, Renaud JB, Schneider-Maunoury S, Shkumatava A, Teboul L, Kent J et al. 2016. Evaluation of off-target and on-target scoring algorithms and integration into the guide RNA selection tool CRISPOR. *Genome Biology* **17**: 148.

Harrison CJ. 2017. Development and genetics in the evolution of land plant body plans. *Philosophical Transactions of the Royal Society of London. Series B: Biological Sciences* **372**: 20150490.

Higo A, Niwa M, Yamato KT, Yamada L, Sawada H, Sakamoto T, Kurata T, Shirakawa M, Endo M, Shigenobu S et al. 2016. Transcriptional framework of male gametogenesis in the liverwort *Marchantia polymorpha* L. *Plant and Cell Physiology* **57**: 325–338.

Hisanaga T, Yamaoka S, Kawashima T, Higo A, Nakajima K, Araki T, Kohchi T, Berger F. 2019. Building new insights in plant gametogenesis from an evolutionary perspective. *Nature Plants* **5**: 663–669.

Hiss M, Meyberg R, Westermann J, Haas FB, Schneider L, Schallenberg-Rudinger M, Ullrich KK, Rensing SA. 2017. Sexual reproduction, sporophyte development and molecular variation in the model moss *Physcomitrella patens*: introducing the ecotype Reute. *The Plant Journal* **90**: 606–620.

Hohe A, Rensing SA, Mildner M, Lang D, Reski R. 2002. Day length and temperature strongly influence sexual reproduction and expression of a novel MADS-box gene in the moss *Physcomitrella patens*. *Plant Biology* **4**: 595–602.

Ito T, Nagata N, Yoshiba Y, Ohme-Takagi M, Ma H, Shinozaki K. 2007. Arabidopsis MALE STERILITY1 encodes a PHD-type transcription factor and regulates pollen and tapetum development. *Plant Cell* **19**: 3549–3562.

Ito T, Shinozaki K. 2002. The MALE STERILITY1 gene of Arabidopsis, encoding a nuclear protein with a PHD-finger motif, is expressed in tapetal cells and is required for pollen maturation. *Plant & Cell Physiology* **43**: 1285–1292.

Kofuji R, Yagita Y, Murata T, Hasebe M. 2018. Antheridial development in the moss *Physcomitrella patens*: implications for understanding stem cells in mosses. *Philosophical Transactions of the Royal Society of London. Series B: Biological Sciences* **373**: 20160494.

Kofuji R, Yoshimura T, Inoue H, Sakakibara K, Hiwatashi Y, Kurata T, Aoyama T, Ueda K, Hasebe M. 2009. Gametangia development in the moss *Physcomitrella patens*. *Annual Plant Reviews* **36**: 167–181.

Kumar S, Stecher G, Li M, Knyaz C, Tamura K. 2018. MEGAX: molecular evolutionary genetics analysis across computing platforms. *Molecular Biology and Evolution* **35**: 1547–1549.

Landberg K, Pederson ERA, Viaene T, Bozorg B, Friml J, Jönsson H, Thelander M, Sundberg E. 2013. The moss *Physcomitrella patens* reproductive organ development is highly organized, affected by the two SHI/STY genes and by the level of active auxin in the SHI/STY expression domain. *Plant Physiology* **162**: 1406–1419.

Landberg K, Šimura J, Ljung K, Sundberg E, Thelander M. 2020. Studies of moss reproductive development indicate that auxin biosynthesis in apical stem cells may constitute an ancestral function for focal growth control. *New Phytologist* **229**: 845–860.

Larkin MA, Blackshields G, Brown NP, Chenna R, McGettigan PA, McWilliam H, Valentin F, Wallace IM, Wilm A, Lopez R et al. 2007. CLUSTALW and CLUSTALX v.2.0. *Bioinformatics* **23**: 2947–2948.

Lei X, Liu B. 2020. Tapetum-dependent male meiosis progression in plants: increasing evidence emerges. *Frontiers in Plant Science* **10**: 1667.

Lopez-Obando M, Hoffmann B, Géry C, Guyon-Debast A, Téoulé E, Rameau C, Bonhomme S, Nogué F. 2016. Simple and efficient targeting of multiple genes through CRISPR-Cas9 in *Physcomitrella patens*. *G3 Genes|Genomes|Genetics* **6**: 3647–3653.

Lopez-Obando M, Landberg K, Sundberg E, Thelander M. 2022. Dependence on clade II bHLH transcription factors for nursing of haploid products by tapetal-like cells is conserved between moss sporangia and angiosperm anthers. *New Phytologist* **235**: 718–731.

Lu JY, Xiong SX, Yin W, Teng XD, Lou Y, Zhu J, Zhang C, Gu JN, Wilson ZA, Yang ZN. 2020. MS1, a direct target of MS188, regulates the expression of key sporophytic pollen coat protein genes in Arabidopsis. *Journal of Experimental Botany* **71**: 4877–4889.

Luo YX, Hou XM, Zhang CJ, Tan LM, Shao CR, Lin RN, Su YN, Cai XW, Li L, Chen S et al. 2020. A plant-specific SWR1 chromatin-remodeling complex couples histone H2A.Z deposition with nucleosome sliding. *EMBO Journal* **39**: e102008.

Mallett DR, Chang M, Cheng X, Bezanilla M. 2019. Efficient and modularCRISPR-Cas9 vector system for *Physcomitrella patens*. *Plant Direct* **3**: e00168.

Meyberg R, Perroud PF, Haas FB, Schneider L, Heimerl T, Renzaglia KS, Rensing SA. 2020. Characterisation of evolutionary conserved key players affecting eukaryotic flagellar motility and fertility using a moss model. *New Phytologist* **227**: 440–454.

Modrzejewski D, Hartung F, Lehnert H, Sprink T, Kohl C, Keilwagen J, Wilhelm R. 2020. Which factors affect the occurrence of off-target effects caused by the use of CRISPR/Cas: a systematic review in plants. *Frontiers in Plant Science* **11**: 574959.

Morris JL, Puttick MN, Clark JW, Edwards D, Kenrick P, Pressel S, Wellmane CH, Yang Z, Schneidera H, Donoghuea PCJ. 2018. The timescale of early land plant evolution. *Proceedings of the National Academy of Sciences, USA* **115**: E2274–E2283.

Motomura K, Arae T, Araki-Uramoto H, Suzuki Y, Takeuchi H, Suzuki T, Ichihashi Y, Shibata A, Shirasu K, Takeda A et al. 2020. AtNOT1 is a novel regulator of gene expression during pollen development. *Plant & Cell Physiology* **61**: 712–721.

Mouriz A, López-González L, Jarillo JA, Piñeiro M. 2015. PHDs govern plant development. *Plant Signaling & Behavior* **10**: e993253.

Notredame C, Higgins DG, Heringa J. 2000. T-COFFEE: a novel method for fast and accurate multiple sequence alignment. *Journal of Molecular Biology* **302**: 205–217.

Ortiz-Ramírez C, Hernandez-Coronado M, Thamm A, Catarino B, Wang M, Dolan L, Feijo JA, Becker JD. 2016. A transcriptome atlas of *Physcomitrella patens* provides insights into the evolution and development of land plants. *Molecular Plant* **9**: 205–220.

Pereira PA, Boavida LC, Santos MR, Becker JD. 2020. AtNOT1 is required for gametophyte development in Arabidopsis. *The Plant Journal* **103**: 1289–1303.

Perroud P-F, Haas FB, Hiss M, Ullrich KK, Alboresi A, Amirebrahimi M, Barry K, Bassi R, Bonhomme S, Chen H et al. 2018. The *Physcomitrella patens* gene atlas project: large-scale RNA-seq based expression data. *The Plant Journal* **95**: 168–182.

Perroud P-F, Meyberg R, Rensing SA. 2019. *Physcomitrella patens* Reute mCherry as a tool for efficient crossing within and between ecotypes. *Plant Biology* **1**(Suppl 1): 143–149.

Potok ME, Wang Y, Xu L, Zhong Z, Liu W, Feng S, Naranbaatar B, Rayatpisheh S, Wang Z, Wohlschlegel JA et al. 2019. Arabidopsis SWR1-associated protein methyl-CpG-binding domain 9 is required for histone H2A.Z deposition. *Nature Communications* **10**: 3352.

Reddy TV, Kaur J, Agashe B, Sundaresan V, Siddiqi I. 2003. The DUET gene is necessary for chromosome organization and progression during male meiosis in Arabidopsis and encodes a PHD finger protein. *Development* **130**: 5975–5987.

Regmi KC, Gaxiola RA. 2017. Alternate modes pf photosynthate transport in the alternating generations of *Physcomitrella patens*. *Frontiers in Plant Science* **8**: 1956.

Reimegård J, Kundu S, Pendle A, Irish VF, Shaw P, Nakayama N, Sundström JF, Emanuelsson O. 2017. Genome-wide identification of physically clustered genes suggests chromatin-level co-regulation in male reproductive development in *Arabidopsis thaliana*. *Nucleic Acids Research* **45**: 3253–3265.

Rensing SA, Weijers D. 2021. Flowering plant embryos: how did we end up here? *Plant Reproduction* **34**: 365–371.

Renzaglia KS, Duff RJ, Nickrent DL, Garbary DJ. 2000. Vegetative and reproductive innovations of early land plants: implications for a unified phylogeny. *Philosophical Transactions of the Royal Society of London. Series B: Biological Sciences* **355**: 769–793.

Sakakibara K, Ando S, Yip HK, Tamada Y, Hiwatashi Y, Murata T, Deguchi H, Hasebe M, Bowman JL. 2013. KNOX2 genes regulate the haploid-to-diploid morphological transition in land plants. *Science* **339**: 1067–1070.

Sakakibara K, Nishiyama T, Deguchi H, Hasebe M. 2008. Class 1 KNOX genes are not involved in shoot development in the moss *Physcomitrella patens* but do function in sporophyte development. *Evolution and Development* **10**: 555–566.

Sanchez-Vera V, Landberg K, Lopez-Obando M, Thelander M, Lagercrantz U, Muñoz-Viana R, Schmidt A, Grossniklaus U, Sundberg E. 2022. The *Physcomitrium patens* egg cell expresses several distinct epigenetic components and utilizes homologues of BONOBO genes for cell specification. *New Phytologist* **233**: 2614–2628.

Schaefer D, Zrÿd J-P, Knight CD, Cove DJ. 1991. Stable transformation of the moss *Physcomitrella patens*. *Molecular and General Genetics* **226**: 418–424.

Schaefer DG, Delacote F, Charlot F, Vrielynck N, Guyon-Debast A, Le Guin S, Neuhaus JM, Doutriaux MP, Nogué F. 2010. RAD51 loss of function abolishes gene targeting and de-represses illegitimate integration in the moss *Physcomitrella patens*. *DNA Repair* **9**: 526–533.

Sharma V, Clark AJ, Kawashima T. 2021. Insights into the molecular evolution of fertilization mechanism in land plants. *Plant Reproduction* **34**: 353–336.

Thelander M, Landberg K, Sundberg E. 2019. Minimal auxin sensing levels in vegetative moss stem cells revealed by a ratiometric reporter. *New Phytologist* **224**: 775–788.

Thelander M, Nilsson A, Olsson T, Johansson M, Girod PA, Schaefer DG, Zryd JP, Ronne H. 2007. The moss genes PpSKI1 and PpSKI2 encode nuclear SnRK1 interacting proteins with homologues in vascular plants. *Plant Molecular Biology* **64**: 559–573.

Wallace IM, O'Sullivan O, Higgins DG, Notredame C. 2006. M-Coffee: combining multiple sequence alignment methods with T-Coffee. *Nucleic Acids Research* **34**: 1692–1699.

Wang J, Niu B, Huang J, Wang H, Yang X, Dong A, Makaroff C, Ma H, Wanga Y. 2016. The PHD finger protein MMD1/DUET ensures the progression of male meiotic chromosome condensation and directly regulates the expression of the condensin gene CAP-D3. *Plant Cell* **28**: 1894–1909.

Wang J, Yu C, Zhang S, Ye J, Dai H, Wang H, Huang J, Cao X, Ma J, Ma H *et al.* 2020. Cell-type-dependent histone demethylase specificity promotes meiotic chromosome condensation in Arabidopsis. *Nature Plants* **6**: 823–837.

Wilson ZA, Morroll SM, Dawson J, Swarup R, Tighe PJ. 2001. The Arabidopsis MALE STERILITY1 MS1 gene is a transcriptional regulator of male gametogenesis, with homology to the PHD-finger family of transcription factors. *The Plant Journal* **28**: 27–39.

Yamaoka S, Nishihama R, Yoshitake Y, Ishida S, Inoue K, Saito M, Okahashi K, Bao H, Nishida H, Yamaguchi K *et al.* 2018. Generative cell specification requires transcription factors evolutionarily conserved in land plants. *Current Biology* **28**: 479–486.

Yang C, Vizcay-Barrena G, Conner K, Wilson ZA. 2007. MALE STERILITY1 is required for tapetal development and pollen wall biosynthesis. *Plant Cell* **19**: 3530–3548.

Yang X, Makaroff CA, Ma H. 2003. The Arabidopsis MALE MEIOCYTE DEATH1 gene encodes a PHD-finger protein that is required for male meiosis. *Plant Cell* **15**: 1281–1295.

Yip HK, Floyd SK, Sakakibara K, Bowman JL. 2016. Class III HD-Zip activity coordinates leaf development in Physcomitrella patens. *Developmental Biology* **419**: 184–197.

Zhou HR, Lin RN, Huang HW, Li L, Cai T, Zhu JK, Chen S, He XJ. 2020. The CCR4-NOT complex component NOT1 regulates RNA-directed DNA methylation and transcriptional silencing by facilitating Pol IV-dependent siRNA production. *The Plant Journal* **103**: 1503–1515.

Supporting Information

Additional Supporting Information may be found online in the Supporting Information section at the end of the article.

Fig. S1 Overviews of how reporter lines were generated.

Fig. S2 Overviews of how *PpMS1A* and *PpMS1B* loss-of-function mutants were generated.

Fig. S3 Data from main Fig. 1(b,c) presented in a way making comparisons of transcript abundance between the two genes possible.

Fig. S4 Amino acid sequence alignment used to infer phylogenetic tree in Fig. 1(a).

Fig. S5 Nonfiltered full length alignment of all proteins in Fig. 1 (a) belonging to the MS1, MMD1, and ancestral MMD1/MS1 subclades.

Fig. S6 Confocal microscopy images showing *PpMS1B:: GFPGUS-1* GFP reporter signals in sporophytes.

Table S1 Primers used in this study.

Table S2 Characteristics of knockout and knock-in lines obtained by CRISPR/CAS9 gene editing.

Table S3 Characteristics of crRNAs in gRNA-expressing plasmids.

Table S4 Average size of inner cells in stage 7 antheridia (harvested 21 dpi).

Table S5 Frequency of phenotypic aberrations in stage 9 archegonia.

Table S6 *Physcomitrium patens* genes for which publicly available RNA-seq data indicates higher expression in green sporophytes, eggs and antheridia, respectively, than in vegetative tissue samples.

Please note: Wiley Blackwell are not responsible for the content or functionality of any Supporting Information supplied by the authors. Any queries (other than missing material) should be directed to the *New Phytologist* Central Office.